Supplementary Materials

IFL/Climate Sensitivity Methods

We regenerated the four layers of climate sensitivity using the R code and MODIS data layers from Seddon et al (2016). In order to extract only forest pixels from these layers, we used Landsat-derived 2000 forest cover produced by Hansen et al (2013) with loss estimates removed and gain estimates added to create a forest cover mask for 2013. This forest mask was resampled to 5 km to match the resolution of the vegetation sensitivity layers and all pixels with a mask value greater than 0.5 were assigned a “1” and exported from Google Earth Engine (Gorelick et al., 2017) to create an inclusive layer of forest cover. Using a combination of QGIS (QGIS Development Team, 2018) and the *raster* package in R (R Development Core Team, 2014), non-forest pixels in the climate sensitivity layers were masked and separate layers of intact and non-intact forest were generated using published shapefiles by Potapov et al (2017) (Figure 1). Finally, intact and non-intact forest pixels were separated into tropical, temperate and boreal biomes using the Olson classifications 1-3, 4 & 5 and 6 respectively derived from the published Anthrome shapefiles (Ellis et al., 2010). To assess differences in sensitivity between intact and non-intact forest pixels by biome, Tukey Honest Statistical Difference values were calculated for all climate metrics. To calculate Tukey HSD values for each region, biome pixels were grouped by longitude ranges. For calculating Tukey HSD values for climate sensitivity of intact forests between regions, regional assignments were extracted from the 2000-2013 IFL shapefile. All statistical analyses were performed in R (R Development Core Team, 2014).

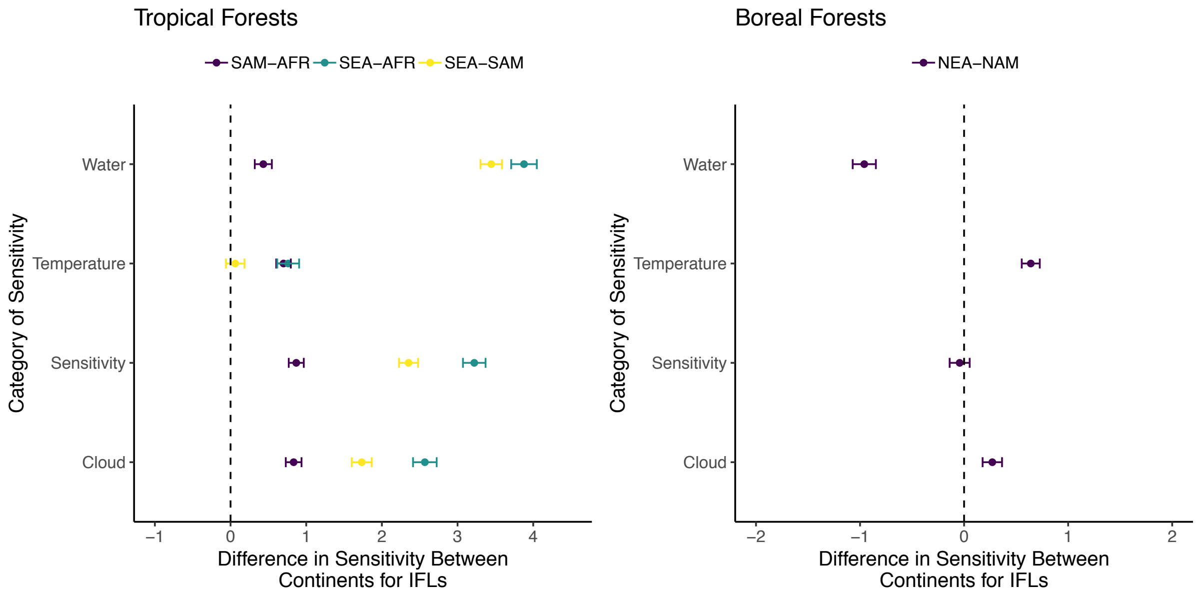

Figure S1 TukeyHSD values, with confidence intervals, comparing climate sensitivity of intact forests, between biome sub-regions in (left) the tropics and (right) boreal forest, for overall sensitivity and temperature, cloud and water sensitivity. Comparison between sub-regions for each biome are reported for Africa (AFR), South America (SAM), Southeast Asia (SEA), North America (NAM) and Northern Europe and Asia (NEA). Negative values indicate intact forest pixels of the first reported sub-region in the legend comparison exhibited lower sensitivity for each variable and positive values indicate the second reported sub-region in the legend comparison exhibited lower sensitivity.

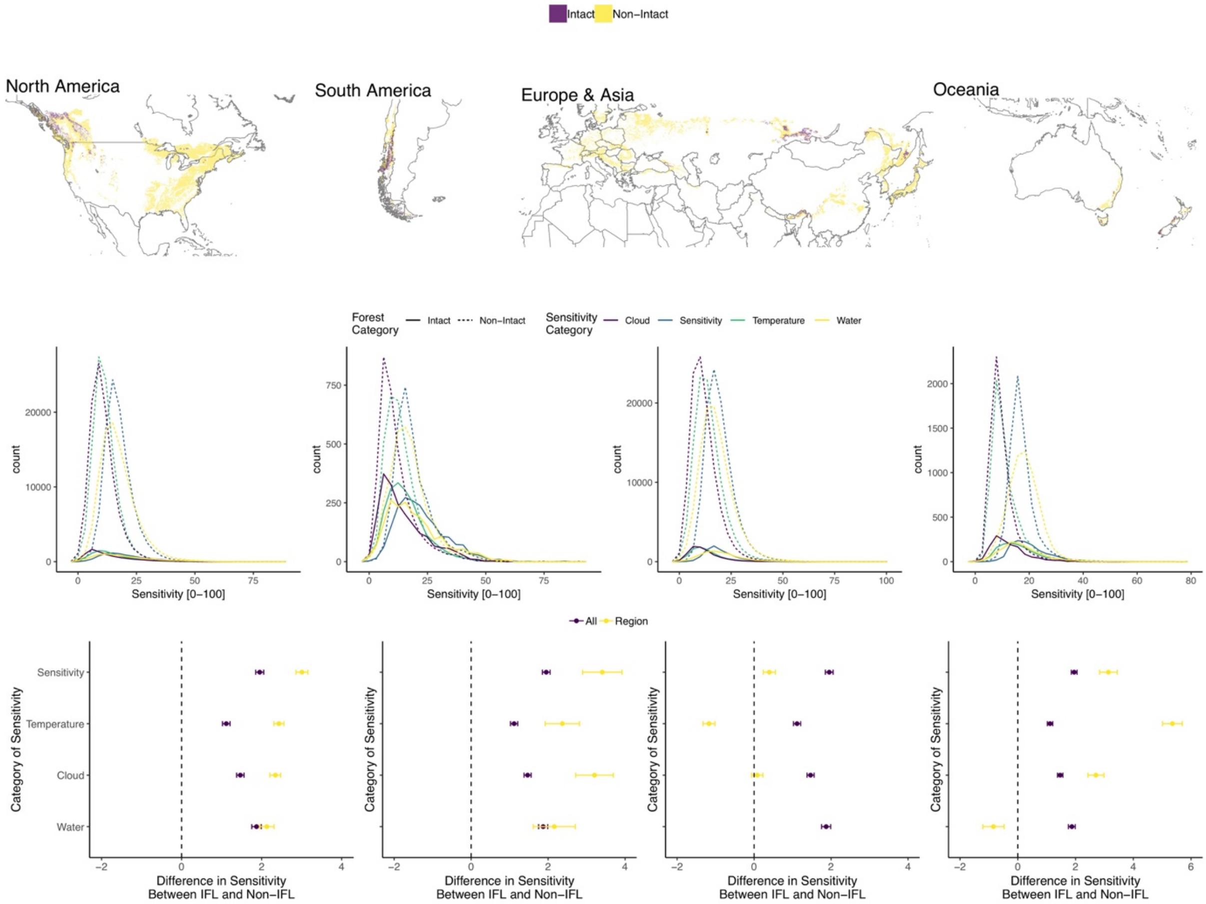

Figure S2 (top row) Distribution of intact and non-intact pixels for each analyzed continent across the temperate biome. (middle row) Histograms of four climate sensitivity metrics for intact (solid) and non-intact (dashed) forests for each continent. (bottom row) TukeyHSD values, with confidence intervals, comparing climate sensitivity of intact and non-intact forests for each climate sensitivity metric for all (“All”) forest pixels across the tropics and for each continent (“Region”). Negative values indicate intact forest pixels exhibited lower sensitivity for each variable and positive values indicate non-intact forest pixels exhibited lower sensitivity.

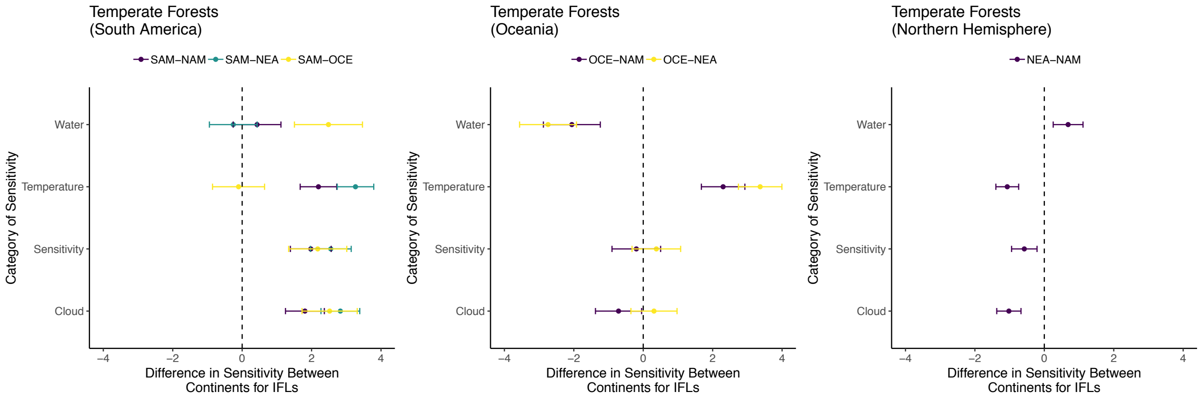

Figure S3 TukeyHSD values, with confidence intervals, comparing climate sensitivity of intact forests, between sub-regions in the temperate zone, for overall sensitivity and temperature, cloud and water sensitivity. Comparison between sub-regions for each biome are reported for South America (SAM), North America (NAM), Oceania (OCE) and Northern Europe and Asia (NEA), separated for clarity. Negative values indicate intact forest pixels of the first reported sub-region in the legend comparison exhibited lower sensitivity for each variable and positive values indicate the second reported sub-region in the legend comparison exhibited lower sensitivity.

References

Ellis, E.C., Klein Goldewijk, K., Siebert, S., Lightman, D., Ramankutty, N., 2010. Anthropogenic transformation of the biomes, 1700 to 2000. Glob. Ecol. Biogeogr. 19, 589–606. https://doi.org/10.1111/j.1466-8238.2010.00540.x

Gorelick, N., Hancher, M., Dixon, M., Ilyushchenko, S., Thau, D., Moore, R., 2017. Google Earth Engine: Planetary-scale geospatial analysis for everyone. Remote Sens. Environ. https://doi.org/10.1016/j.rse.2017.06.031

Hansen, M.C., Potapov, P.V., Moore, R., Hancher, M., Turubanova, S.A., Tyukavina, A., S. V. Stehman, S. J. Goetz, T. R. Loveland, A. Kommareddy, A. Egorov, L. Chini, C. O. Justice, J. R. G. Townshend, 2013. High-Resolution Global Maps of 21st-Century Forest Cover Change. Science 342, 850–853.

Potapov, P., Hansen, M.C., Laestadius, L., Turubanova, S., Yaroshenko, A., Thies, C., Smith, W., Zhuravleva, I., Komarova, A., Minnemeyer, S., Esipova, E., 2017. The last frontiers of wilderness: Tracking loss of intact forest landscapes from 2000 to 2013. Sci. Adv. 3. https://doi.org/10.1126/sciadv.1600821

QGIS Development Team, 2018. QGIS Geographic Information System. Open Source Geospatial Foundation Project.

R Development Core Team, 2014. R: A language and environment for statistical computing. R Found. Stat. Comput.

Seddon, A.W.R., Macias-Fauria, M., Long, P.R., Benz, D., Willis, K.J., 2016. Sensitivity of global terrestrial ecosystems to climate variability. Nature 531, 229. https://doi.org/10.1038/nature16986